GEO-REFERENCING AND STEREO CALIBRATION OF GROUND-BASED WHOLE SKY IMAGERS USING THE SUN TRAJECTORY

Florian M. Savoy[1], *Soumyabrata Dev*[2], *Yee Hui Lee*[2], *Stefan Winkler*[1]

[1] Advanced Digital Sciences Center, University of Illinois at Urbana-Champaign, Singapore
[2] School of Electrical and Electronic Engineering, Nanyang Technological University, Singapore

ABSTRACT

Ground-based Whole Sky Imagers (WSIs) are now commonly used for cloud observations. Upon deployment, they may not be exactly level or precisely face north. This significantly affects subsequent processing of the images, especially for applications where two or more imagers are required, e.g. 3D volumetric cloud reconstruction.

We present a method to remove this mis-alignment using the sun position in images captured over a whole day. Coupled with precise coordinates of the device locations, this method also improves the geo-referencing accuracy of the captured images. We detect the sun in the images and compute the corresponding 3D vectors using the lens calibration function. These vectors are compared to the actual sun direction. The mismatch between the two sets of vectors is then corrected using a 3D rotation matrix. The method can also be applied to other celestial bodies, such as stars or the moon.

***Index Terms*—** WAHRSIS, ground-based sky camera, Whole Sky Imager (WSI), stereo calibration, geo-referencing

1. INTRODUCTION

Localized cloud monitoring using ground-based imagers is becoming popular for a variety of applications and domains, such as solar energy generation, satellite communications, and weather prediction. We designed our own custom made Whole Sky Imagers (WSIs), which we call WAHRSIS (Wide Angle High Resolution Sky Imaging System) [1, 2]. They consist of a DSLR camera with a hemispherical fish-eye lens in a weather-proof enclosure and capture images at regular intervals controlled by a single board computer.

In practice, aligning the imagers is not an easy task. They should be perfectly oriented towards the north and lie horizontally. Quantifying the mis-alignments is crucial for tasks such as volumetric cloud reconstruction, where pictures from more than one WSIs need to be matched for triangulation. The mis-alignments of each imager have a significant impact in the accuracy of the triangulation and thus need to be corrected. In an earlier paper [3] on 3D cloud reconstruction based on scene flow, we *manually* compensated for mis-alignments, which is tedious. Further aggrevating this problem is that we frequently open the enclosure and move the camera inside our sky imagers for maintenance or testing purposes. The camera position inside the enclosure is also not perfectly aligned and has a small degree of freedom. This led us to developing a software-based calibration approach.[1]

We use the sun as a reference. It is visible by every imager, and its precise position is known. Due the large distance of the sun from both imagers, we assume that it should be captured at the same pixel location in two perfectly aligned imagers. We use the difference between the detected positions in each misaligned imager and the ground truth provided by astronomical equations to compute device-dependent correction factors in the form of a 3D rotation matrix.

Since we use the true position of the sun, the proposed technique does not only correct for mis-alignments relative to the imagers themselves, but also aligns the images to earth coordinates. The vertical axis of each corrected image becomes parallel to the meridian, and the ray passing through its center point is perpendicular to the earth surface. This allows the results of subsequent 3D reconstruction algorithms to be accurately geo-referenced, provided that a precise location of the devices is available.

Similar to the sun, the positions of the moon or stars could also be used. The moon is easily detectable in night images, but this is challenging during daytime. Furthermore, its phases make precise location estimation difficult. Stars are harder to detect due to their low luminance and small size in the images. Their distribution across the entire sky would however provide more uniformly sampled points as input to the algorithm.

The paper is organized as follows: after this introduction, related works are discussed in Section 2. Our approach is presented in Section 3, with a discussion of the results in Section 4. Section 5 concludes the paper.

This research is funded by the Defence Science and Technology Agency (DSTA), Singapore.

Send correspondence to `Stefan.Winkler@adsc.com.sg`.

[1] Note that the device mis-alignments discussed in this paper are different from traditional camera calibration [1], which relates pixel locations to incident light rays for an individual camera.

2. RELATED WORKS

Most papers about cloud base height or 3D reconstruction assume the devices to be physically aligned. To the best of our knowledge, only two publications present details about similar calibration and correction procedures. Seiz et al. [4] use the positions of the stars at night as a reference. Their contribution combines both lens calibration and mis-alignment correction, while our proposed method differentiates both. Gauchet et al. [5] also use the sun as a reference. However, no details are provided about their calibration procedure.

In the general context of stereoscopic depth estimation with standard lenses, Zhao and Nandhakumar [6] analyzed the effects of various mis-alignments such as roll, pitch and yaw to specify an acceptable range for such errors. Ding et al. [7] derived depth estimation formulas incorporating different and composite sources of mis-alignment, estimating them using a feature matching based method. Santoro et al. [8] propose a mis-alignement correction method to cope with camera shift using motion estimation.

3. CALIBRATION ALGORITHM

We model the mis-alignment error as a 3D rotation matrix, which is applied on the unit vectors representing the incident light rays of each pixels. The behavior of the lens is modeled by the invertible lens calibration function, which relates pixel positions to incident light rays on the unit sphere.

We use all the images taken over a day and automatically detect the sun position in them. Since the exact azimuth and elevation angles of the sun are known, we compute the optimal rotation matrix mapping the detected positions to the positions where the sun is supposed to be without mis-alignments. We finally apply this matrix on the light rays of every pixel to calibrate the images. Each imager is processed independently, as their mis-alignments are different.

3.1. Camera Calibration

Our sky imagers use *SIGMA 4.5mm F2.8 EX DC* circular fisheye lenses. Those are designed to follow the equisolid equation:

$$r = c \cdot \sin(\theta/2)$$

where r described the distance from the image center, θ the angle from the optical axis and c a constant.

Through standard camera calibration [1], we found this model to capture the characeristics of our lens very accurately. In our setup, $c = 1472$ for an image resolution of 5184×3456 pixels. The azimuth angle being unchanged, this equation is sufficient to map each pixel location to its incident light ray. The relationship between pixel positions in the image to incident light rays on the unit sphere is illustrated in Figure 1.

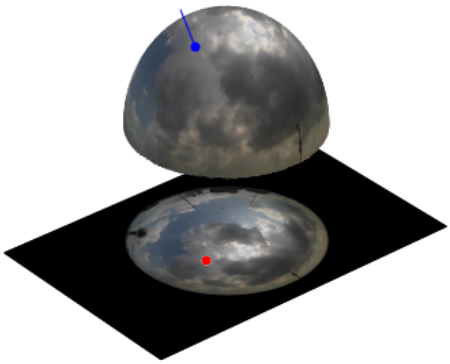

Fig. 1: The input image is shown at the bottom, with a pixel highlighted in red. The corresponding unit hemisphere is shown on top, which each pixel plotted where its incident light ray intersects the hemisphere. The incident light ray from that red pixel is shown in blue, with a point at the unit length vector.

3.2. Sun Detection

The sun moves across the hemisphere every day. However, its detection is harder in standard-exposure Low Dynamic Range (LDR) images. Our Whole Sky Imagers capture several successive LDR shots with different camera settings as inputs to compute High Dynamic Range (HDR) images. It is then easier to detect the sun in the lowest luminosity LDR image.

Our sky imagers capture three LDR images with varying exposures. We use the lowest luminosity one, captured with a -4EV setting, as shown in Fig. 2. We see that the sun is the only bright spot visible in the image.

Fig. 2: Low luminosity LDR image captured by WAHRSIS.

The position of the sun is detected by thresholding. We experimentally set the threshold as 240 in the red channel. The sun location is then computed as the centroid of the largest area with pixel values above the threshold. When the sun is temporarily blocked by clouds, no such area may be detected, in which case we skip the image.

3.3. Polynomial Regression of the Sun Trajectory

The sun detection algorithm is not perfect, especially when the sun is partially covered by clouds, as shown in Fig. 3(b).

In order to cope with these inaccuracies, we fit a cubic polynomial to the set of detected image coordinates of the sun, as shown in Fig. 4. We uniformly sample points along that curve. This technique relies on the fact that the sun follows a smooth trajectory.

(a) Cloud-free conditions (error of 0.007 pixels)

(b) Cloudy sky (error of 220 pixels)

Fig. 3: Detection of the sun in (a) cloud-free and (b) cloudy conditions. The detected sun location is shown in red.

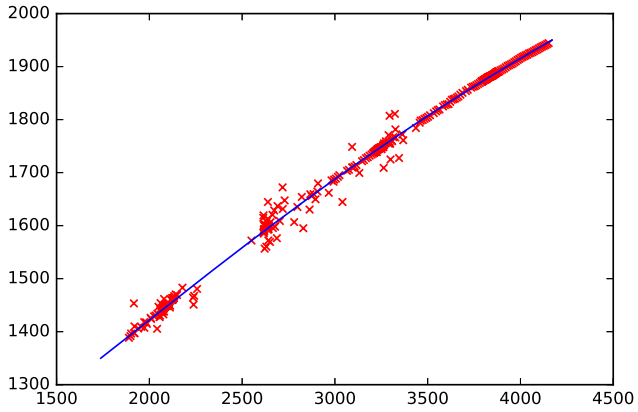

Fig. 4: Detected points (in image coordinates) as red crosses and fitted curve in blue.

3.4. Rotation Matrix

The physical position of the sun can be computed using the formulas in [9], providing date, time, and location as input. Using the algorithm detailed above and the lens calibration function, we compute the incident light rays of the detected sun positions for images taken over a whole day at two-minute intervals. These rays are different from the ground truth rays, as they reflect the orientation mismatch of the imager. We compute the 3D rotation matrix which best transforms this set of rays to the ground truth. For this purpose, we use the iterative closest point (ICP) method from [10]. One separate rotation matrix is computed for each imager.

In order to remove the mis-alignment effect from an image, we convert each of its pixels to unit vectors in 3D using the lens calibration function. We then apply the rotation matrix and convert them back to 2D pixel locations.

4. RESULTS

Figure 5 shows the trajectories of the sun in the image plane, with the detected sun locations in blue, and the location after correction in green. The mismatch of the blue and green lines clearly indicates the relative mis-alignment of the two imagers, while the locations after successful correction (in green) are in the same place in both images. The missing parts along the curves are due to clouds covering the sun.

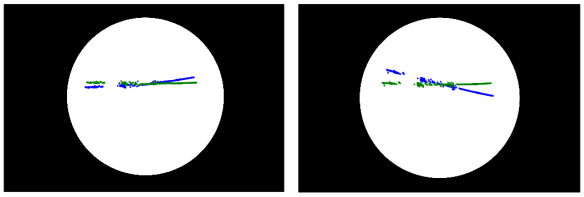

(a) First imager

(b) Second imager

Fig. 5: Trajectories of the sun on the captured images across one day for both imagers. The detected sun locations are shown in blue. Sun locations after applying the correction are plotted in green.

The root-mean-square error (RMSE) of the distance between detected location and ground truth is 179.8 pixels in the example shown in Figure 5 (minimum: 35 pixels, maximum 288 pixels). Applying the rotation matrix reduces RMSE significantly to 18.2 pixels (minimum: 4 pixels, maximum: 81 pixels), which corresponds to an angular error of about 0.9 degrees. Figure 6 shows those errors as a function of the time of day. Inspection of the images reveals that clouds were present from 11.30am onward, with a rain event between 3.15pm and 4pm. This translates to larger detection errors and missing points during that period.

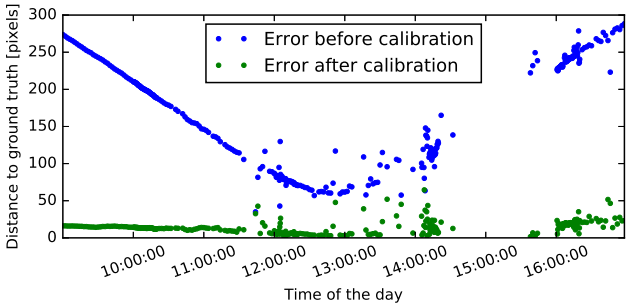

Fig. 6: Error (distance in pixels from the ground truth location) before (blue dots) and after (green dots) the correction.

Figure 7 shows an overlay of images captured at the same time by two imagers 100 meters apart both without and with

correction by the rotation matrices. We can observe that the positions of the sun differ without applying the correction, whereas the sun appears essentially in the same place after the correction.

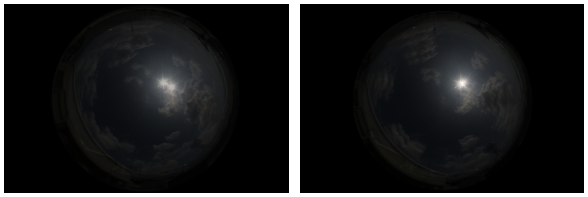

(a) Before correction (b) After correction

Fig. 7: Overlay of images captured at the same time by two imagers 100 meters apart (a) before and (b) after correction.

5. CONCLUSIONS

We presented a software-based calibration method for correcting positioning mis-alignments of Whole Sky Imagers and providing accurate geo-referenceing of the captured images. We use the sun as a reference, which we detect via simple thresholding.

Our future work includes the use of the moon or stars as a reference, as well as studying the effects of irregular sampling of the image due to clouds covering the sun and possible imprecisions resulting from the sun trajectory only passing through a small part of the hemisphere.

6. REFERENCES

[1] S. Dev, F. M. Savoy, Y. H. Lee, and S. Winkler, "WAHRSIS: A low-cost, high-resolution whole sky imager with near-infrared capabilities," in *Proc. IS&T/SPIE Infrared Imaging Systems: Design, Analysis, Modeling, and Testing*, 2014.

[2] S. Dev, F. M. Savoy, Y. H. Lee, and S. Winkler, "Design of low-cost, compact and weather-proof whole sky imagers for high-dynamic-range captures," in *Proc. IEEE International Geoscience and Remote Sensing Symposium (IGARSS)*, 2015, pp. 5359–5362.

[3] F. M. Savoy, J. C Lemaitre, S. Dev, Y. H. Lee, and S. Winkler, "Cloud base height estimation using high-resolution whole sky imagers," in *Proc. IEEE International Geoscience and Remote Sensing Symposium (IGARSS)*, 2015.

[4] G. Seiz, E. P. Baltsavias, and A. Gruen, "Cloud mapping from the ground: Use of photogrammetric methods," *Photogrammetric Engineering and Remote Sensing*, vol. 68, no. 9, pp. 941–951, 2002.

[5] C. Gauchet, P. Blanc, B. Espinar, B. Charbonnier, and D. Demengel, "Surface solar irradiance estimation with low-cost fish-eye camera," in *Proc. Workshop on Remote Sensing Measurements for Renewable Energy*, 2012.

[6] W. Zhao and N. Nandhakumar, "Effects of camera alignment errors on stereoscopic depth estimates," *Pattern Recognition*, vol. 29, no. 12, pp. 2115–2126, 1996.

[7] X. Ding, L. Xu, H. Wang, X. Wang, and G. Lv, "Stereo depth estimation under different camera calibration and alignment errors," *Applied Optics*, vol. 50, no. 10, pp. 1289–1301, 2011.

[8] M. Santoro, G. AlRegib, and Y. Altunbasak, "Misalignment correction for depth estimation using stereoscopic 3-D cameras," in *Proc. 14th IEEE International Workshop on Multimedia Signal Processing (MMSP)*, 2012, pp. 19–24.

[9] J. H. Meeus, *Astronomical Algorithms*, Willmann-Bell, 1991.

[10] P. J. Besl and N. D. McKay, "A method for registration of 3-D shapes," *IEEE Transactions on Pattern Analysis and Machine Intelligence*, vol. 14, no. 2, pp. 239–256, 1992.